Topological edge states in periodically-driven trapped-ion chains

Article (Published Version)

Nevado, Pedro, Fernandez-Lorenzo, Samuel and Porras, Diego (2017) Topological edge states in periodically-driven trapped-ion chains. Physical Review Letters, 119 (210401). ISSN 0031-9007

Topological Edge States in Periodically Driven Trapped-Ion Chains

Pedro Nevado,* Samuel Fernández-Lorenzo, and Diego Porras†
Department of Physics and Astronomy, University of Sussex, Brighton BN1 9QH, United Kingdom

(Received 14 June 2017; revised manuscript received 18 September 2017; published 20 November 2017)

Topological insulating phases are primarily associated with condensed-matter systems, which typically feature short-range interactions. Nevertheless, many realizations of quantum matter can exhibit long-range interactions, and it is still largely unknown the effect that these latter may exert upon the topological phases. In this Letter, we investigate the Su-Schrieffer-Heeger topological insulator in the presence of long-range interactions. We show that this model can be readily realized in quantum simulators with trapped ions by means of a periodic driving. Our results indicate that the localization of the associated edge states is enhanced by the long-range interactions, and that the localized components survive within the ground state of the model. These effects could be easily confirmed in current state-of-the-art experimental implementations.

DOI: 10.1103/PhysRevLett.119.210401

Introduction.—Topological phases are one of the most exotic forms of quantum matter. Among their many intriguing traits, we find that they are robust against local decoherence processes, or feature fractional particle excitations with prospective applications in quantum information processing [1,2]. Some of the simplest systems showcasing nontrivial topological order are the topological insulators [3–6], gapped phases of noninteracting fermions which present gapless edge states. Despite several experimental realizations [7,8], the preparation and measurement of topological insulators is typically difficult in the solid state. Analog quantum simulators [9–15], on the other hand, offer the possibility of exploring and exploiting the topological insulating phases, because of their inherent high degree of controllability. Furthermore, interactions in a quantum simulator can be tuned at will, opening up the possibility of investigating new regimes of the underlying models.

Topological edge states usually occur in the insulating phase as long as an associated bulk invariant attains a nontrivial value, and the generic symmetries of the underlying Hamiltonian are preserved [16]. This property—known as the bulk-edge correspondence—is a generic feature of topological insulators. However, if interactions are taken into account, the presence of edge states is no longer guaranteed. For instance, it has been shown that one of the edge states present in the Mott insulating phase of the Bose-Hubbard model on a 1D superlattice is not stable against tunneling [17]. In this work, we extend these considerations to the case of interactions which are explicitly long ranged. Since topological phases are characteristically robust against *local* perturbations, but long-range interactions may not qualify as such, there is an ongoing effort to elucidate their effect upon the topological states [18–20]. This question is not of exclusive theoretical interest, since many experimental systems implementing topological phases of matter feature long-range interactions. In particular, we will show that trapped-ion quantum simulators can realize a long-range interacting version of one of the simplest instances of a topological insulator, the Su-Schrieffer-Heeger (SSH) model [21–23]

$$H_{\mathrm{SSH}} = J\sum_{j=1}^{N-1}[1+\delta(-1)^j](\sigma_j^+\sigma_{j+1}^- + \mathrm{H.c.}). \quad (1)$$

The SSH model presents topological edges states for $\delta > 0$, which, e.g., near the left end of the chain are of the form $|\mathrm{E.S.}\rangle \sim \sum_{j=1}^{N} e^{(N-j+1)/\xi_{\mathrm{loc}}}\sigma_j^+|\downarrow\downarrow\downarrow\ldots\rangle$, where the localization length can be related to the dimerization δ through [24]

$$\xi_{\mathrm{loc}} = -2/\ln\frac{1-\delta}{1+\delta}, \qquad 0<\delta<1. \quad (2)$$

The addition of long-range interion couplings on Eq. (1) turns this model into a highly nontrivial interacting problem. However, we will show that, owing to the single-particle addressability available in trapped-ion setups, the edge states can be studied as one-body solutions, and that their properties survive when interactions are taken into account.

This Letter is structured as follows. (i) We begin showing how to implement the interacting SSH model with trapped-ion quantum matter. (ii) We then study its one-excitation subspace, and locate the topological phase. (iii) We perform an effective description of the low-energy sector, and establish the dependence of the localization length with the range of the interactions. Also, we provide a protocol for the detection of the edge states. (iv) Finally, we study the correlations in the ground state, and establish the survival of the boundary modes against interactions.

Realization of the spin SSH Hamiltonian.—We consider a set of N trapped ions arranged along a 1D chain. Two optical or hyperfine levels $|\uparrow\rangle, |\downarrow\rangle$ encode an effective spin, such that $|\uparrow\rangle\langle\uparrow| - |\downarrow\rangle\langle\downarrow| \equiv \sigma^z$ [25]. The vibrations of the chain can be approximated by a set of harmonic modes, $H_{\mathrm{ph}} = \sum_{n=1}^{N}\omega_n a_n^\dagger a_n$. We add a state-dependent force conditional on the internal states of the ions [26–29], whose frequency is fairly off-resonant with any motional excitation,

$$H_f(t) = g \sum_{j,n=1}^{N} \sigma_j^x (M_{j,n} e^{i\delta_n t} a_n^\dagger + \text{H.c.}), \quad (3)$$

$\delta_n = \omega_n - \Delta\omega$, where $\Delta\omega$ is the laser detuning with respect to the internal level and $M_{j,n}$ is the phonon wave function. We assume that the force acts in the direction transverse to the ion chain. In this case the mode $n = N/2$ has the minimum energy. After tracing out the vibrational bath, the dynamics of the spins can be described by an Ising Hamiltonian [11],

$$H_{\text{Ising}} = \sum_{j,l=1}^{N} J_{j,l}^{(\text{ions})} \sigma_j^x \sigma_l^x + \frac{\Omega}{2} \sum_{j=1}^{N} \sigma_j^z, \quad (4)$$

where the extra transversal field Ω can be realized with a microwave or a Raman transition. The nature of the couplings $J_{j,l}^{(\text{ions})}$ depends on the width of the dispersion relation of the motional modes t_C and the detuning of the laser from the bottom of the band, $\delta_{N/2}$ [30]. All through this work we assume $\delta_{N/2} > 0$. In Ref. [31] we showed that depending on the relative values of $\delta_{N/2}$ and t_C, we can distinguish two regimes: (i) the long-range limit ($\delta_{N/2} \ll t_C$), in which $J_{j,l}^{(\text{ions})} \sim e^{-|j-l|/\xi_{\text{int}}}$. The spin coupling takes a Yukawa-like form, with $\xi_{\text{int}} = \sqrt{\log(2)/2}\sqrt{t_C/\delta_{N/2}}$, and (ii) short-range limit ($\delta_{N/2} \gg t_C$), in which the couplings decay as $\sim|j-l|^{-3}$, and the interactions are effectively among nearest neighbors only.

Since $\sigma_j^x = \sigma_j^+ + \sigma_j^-$, Hamiltonian (4) contains terms of the form $\sigma_j^+\sigma_l^+$, $\sigma_j^-\sigma_l^-$, which do not occur in Eq. (1). To eliminate these we assume a rotating wave approximation in the limit $\Omega \gg J_{j,l}$. To obtain the SSH model we consider driving the chain with a time-dependent field. Periodic drivings are known to render effective Hamiltonians in which specific terms can be adiabatically eliminated, and the interactions are nontrivially dressed [32]. In our case, this dressing must also contain some spatial structure to give rise to the periodicity of the couplings in the SSH model. We exploit the possibility of globally imprinting inhomogeneous couplings upon the chain, by taking advantage of the optical phase of the laser fields [31],

$$H_{\text{driving}} = \frac{\eta\omega_d}{2} \cos(\omega_d t) \sum_{j=1}^{N} \cos(\Delta k d_0 j + \phi) \sigma_j^z. \quad (5)$$

This driving relies on a standing wave modulated in time with frequency $\omega_d \ll \Omega$, which should be implemented by a different set of lasers than the state-dependent force in Eq. (3). η is the (dimensionless) coupling strength, Δk is the wave vector along the chain axis, and ϕ is a global optical shift. We assume that the ions are equally spaced by d_0, so their equilibrium positions are $r_j^{(0)} = d_0 j$. This is a good approximation in the center of a Coulomb crystal in a rf trap [33], or describes a linear array of microtraps [34–36]. Now we move into a rotating frame such that $H_{\text{Ising}} + H_{\text{driving}} \equiv H_{\text{total}} \to H'_{\text{total}}$, with $H'_{\text{total}} = U(t) H_{\text{total}} U^\dagger(t) - iU(t)(d/dt)U^\dagger(t)$, $U(t) = \exp[i \sum_{j=1}^{N} \Delta_j(t) \sigma_j^z]$, and

$$\Delta_j(t) = \frac{\Omega}{2} t + \frac{\eta\omega_d}{2} \cos(\Delta k d_0 j + \phi) \int_0^t \cos(\omega_d t') dt'. \quad (6)$$

The condition $\max_{j,l}|J_{j,l}^{(\text{ions})}| \ll \Omega$ ensures that the anomalous terms are fast rotating, whereas those that preserve the z component of the spin are renormalized by the phases $e^{\pm i[\Delta_j(t) - \Delta_l(t)]}$. These quantities can be simplified by using suitable trigonometric identities along with the Jacobi-Anger expansion $e^{iz\sin\theta} = \sum_{n=-\infty}^{\infty} B_n(z) e^{in\theta}$, where $B_n(z)$ are the Bessel functions of the first kind [37]. Assuming that $\omega_d \gg \max_{j,l}|J_{j,l}^{(\text{ions})}|$, the only non-fast-rotating contribution comes from $n = 0$, and $H'_{\text{total}} \simeq H_{\text{SSH}}^{(\text{ions})}$, with

$$H_{\text{SSH}}^{(\text{ions})} = \sum_{j,l=1}^{N} J_{j,l}^{(\text{ions})} \mathcal{J}_{j,l}^{\pi/2} (\sigma_j^+ \sigma_l^- + \sigma_j^- \sigma_l^+), \quad (7)$$

where we fix $\Delta k d_0 = \pi/2$ to achieve the periodic couplings

$$\mathcal{J}_{j,l}^{\pi/2} = B_0\left[2\eta \sin\left(\frac{\pi}{4}(j+l) + \phi\right) \sin\frac{\pi}{4}(j-l)\right]. \quad (8)$$

Since $\mathcal{J}_{j,j+1}^{\pi/2} = \mathcal{J}_{j+T,j+T+1}^{\pi/2}$ with $T = 2$, these couplings reproduce the dimerization of the original SSH model in the limit of nearest-neighbor interactions. We will refer to the spin implementation (7) as the generalized SSH model. In analogy with Eq. (1), the dimerization is given by the differential ratio of the couplings between sites with j even and odd, i.e.,

$$\delta = \frac{\mathcal{J}_{2,3}^{\pi/2} - \mathcal{J}_{1,2}^{\pi/2}}{\mathcal{J}_{2,3}^{\pi/2} + \mathcal{J}_{1,2}^{\pi/2}}. \quad (9)$$

In Eq. (9), $J_{j,l}^{(\text{ions})}$ factors out, since $J_{j,l}^{(\text{ions})} = J_{j-l}^{(\text{ions})}$.

Finally, we remark that we can easily extend our derivation to account for the effect of an inhomogeneous ion-ion spacing, whose main effect would be to induce an extra site dependence in the couplings to the standing wave. Since the topological properties investigated below are robust against perturbations, we can expect our results to be valid even when small inhomogeneities are considered.

Study in the one-excitation subspace.—The preparation of single excitations can be easily realized in trapped-ion chains, as demonstrated in implementations of the Ising and XY models [14,15]. The one-particle sector is spanned by the vectors $|j\rangle \equiv \sigma_j^+|\downarrow\downarrow\downarrow\cdots\rangle$, $j = 1, \ldots, N$. We can think of the state $|\downarrow\downarrow\downarrow\cdots\rangle$ as a vacuum of particles, and, accordingly, $|j\rangle$ represents an excitation localized at site j. Since Eq. (7) is invariant under arbitrary rotations in the xy plane, the Hamiltonian does not mix $|j\rangle$ with states within subspaces of different numbers of excitations.

Therefore, the dynamics of $|j\rangle$ is dictated by the restriction of the Hamiltonian to the one-excitation subspace, that is given as

$$\bar{H}_{\mathrm{SSH}}^{(\mathrm{ions})} = \sum_{j,l=1}^{N} h_{j,l}(|j\rangle\langle l| + |l\rangle\langle j|), \qquad h_{j,l} = J_{j,l}^{(\mathrm{ions})}\mathcal{J}_{j,l}^{\pi/2}. \tag{10}$$

For $\phi = 3\pi/4$ and $\eta > 0$, $h_{j,l}$ possesses two (quasi-) zero-energy modes, which feature localization at the edges; we show one of these in Fig. 1(a). The edge state has appreciable support only on the odd sites, which is a consequence of the chiral symmetry [38]. Indeed, the chiral-symmetric limits of this Hamiltonian are attained for $\phi = \pi/4$ and $3\pi/4$ (see Ref. [39]). We have depicted the dimerization (9) as a function of η in these limits [cf. Fig. 1(b)]. We note that for $\phi = 3\pi/4$, δ is positive, and accordingly the model presents edge states. This is accompanied by a nonzero value of the associated bulk invariant, the Zak phase [46], which can take the value $0(\pm\pi)$ in the trivial (topological) phase. As shown in Fig. 1(c), the Zak phase is 0 or $\pm\pi$ in the chiral limits $\phi = \pi/4$ and $\phi = 3\pi/4$, signaling the emergence of edge states in this latter case.

By fitting the edge state to an exponential, we can estimate its localization length numerically. According to Eq. (2), this quantity is a decreasing function of the dimerization. This holds true for $\bar{H}_{\mathrm{SSH}}^{(\mathrm{ions})}$, as shown in Fig. 1(d). However, we note that ξ_{loc} decreases with the range of the interactions as well; i.e., there is an enhancement of the localization effect. This feature is not captured by the prediction for the original

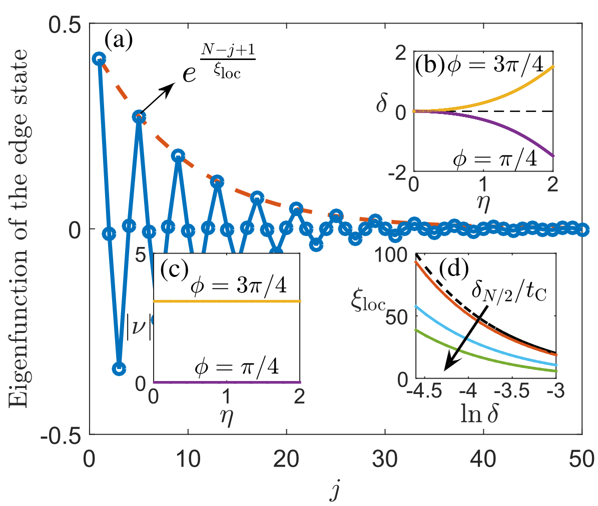

FIG. 1. (a) Plot of the midgap state (circles) near the left end, with $\delta_{N/2}/t_C = 4$, for $N = 100$, $\delta \simeq 0.1$ ($\phi = 3\pi/4$, $\eta \simeq 0.62$). The solid line is a guide for the eye, and the dashed curve is the envelope of the edge state. (b) Dimerization as a function of η in the chiral limits. (c) Zak phase for different values of η, signaling the topologically trivial ($|\nu| = 0$) and nontrivial ($|\nu| = \pi$) phases. (d) Dependence of ξ_{loc} with the dimerization, for $\delta_{N/2}/t_C = 0.1$, 0.5, 8. The dashed line corresponds to Eq. (9).

SSH model, since ξ_{loc} exclusively depends on δ, and this latter quantity is insensitive to the range of the couplings [cf. Eq. (9)]. To obtain the dependence of the localization on the interaction range we have considered the effective theory for the low-energy sector of $\bar{H}_{\mathrm{SSH}}^{(\mathrm{ions})}$, which captures the long-range effects by a renormalization of the parameters of the theory compared to those of the original SSH model.

Localization length of the edge states of $\bar{H}_{\mathrm{SSH}}^{(\mathrm{ions})}$.—The effective theory of the SSH model in k space can be described in terms of pairs of states $|k,\pm\rangle = |k \pm k_F\rangle$, where $k_F \equiv \pi/2$. The low energy Hamiltonian is given by $H_{\mathrm{low}E} = (N/2\pi)\int_{-\pi/2}^{\pi/2} h(k)dk$, with

$$h(k) = kv_F(|k,+\rangle\langle k,+| - |k,-\rangle\langle k,-|) - i\Delta_0(|k,+\rangle\langle k,-| - |k,-\rangle\langle k,+|). \tag{11}$$

The two parameters $v_F = 2J$ and $\Delta_0 = 2J\delta$ fully characterize the low energy sector. From them, the dimerization is directly obtained as $\Delta_0/v_F = \delta$, and since the effective theory assumes that $\Delta_0 \ll v_F$, we can approximate the localization length (2) as

$$\xi_{\mathrm{loc}} \sim \frac{v_F}{\Delta_0}. \tag{12}$$

This prediction must hold for any lattice model whose low-energy excitations are captured by a Hamiltonian such as $H_{\mathrm{low}E}$. In particular, this is the case for $\bar{H}_{\mathrm{SSH}}^{(\mathrm{ions})}$, that can be rewritten as $\sum_{j=1}^{N}\sum_{d=1-j}^{N-j} h_j^{(d)}(|j\rangle\langle j+d| + |j+d\rangle\langle j|)$, where $h_j^{(d)} \equiv J_d^{(\mathrm{ions})}[\mathcal{J}_d^{(+)} + \mathcal{J}_d^{(-)}(-1)^j]$, with

$$\mathcal{J}_d^{(\pm)} = \frac{1}{2}(\mathcal{J}_d^{\mathrm{even}} \pm \mathcal{J}_d^{\mathrm{odd}}), \tag{13}$$

and the latter quantities defined as $\mathcal{J}_{j,j+d}^{\pi/2}$ for j even or odd, respectively. In terms of plane waves, and assuming $N \to \infty$, we obtain

$$\bar{H}_{\mathrm{SSH}}^{(\mathrm{ions})} = \sum_k \varepsilon'(k)|k\rangle\langle k| + \sum_k \Delta'(k)|k+\pi\rangle\langle k| + \mathrm{H.c.}, \tag{14}$$

where we have defined

$$\varepsilon'(k) = 4\sum_{d=1}^{\infty} J_d^{(\mathrm{ions})}\mathcal{J}_d^{(+)}\cos(kd),$$

$$\Delta'(k) = 2\sum_{d=1}^{\infty} J_d^{(\mathrm{ions})}\mathcal{J}_d^{(-)}e^{ikd}. \tag{15}$$

From these quantities, we can obtain the parameters of the effective theory as (see Ref. [39])

$$v_F' = \left.\frac{\partial\varepsilon'(k)}{\partial k}\right|_{k=k_F}, \qquad \Delta_0' = 2\mathrm{Im}[\Delta'(k=k_F)], \tag{16}$$

and compute the localization length (12). We show that this prediction accurately holds for several values of $\delta_{N/2}/t_C$ in

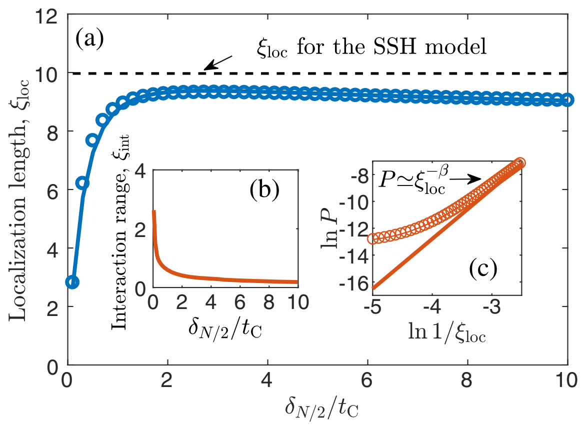

FIG. 2. (a) Localization length of the edge state, from the exact diagonalization of $\bar{H}_{\rm SSH}^{\rm (ions)}$ (solid line) for $N = 100$ sites, and from expression (12) (circles) with $\delta = 0.1$ ($\phi = 3\pi/4$, $\eta \simeq 0.62$). The largest enhancement of $\xi_{\rm loc}$ occurs for $\delta_{N/2}/t_C < 1$. (b) Interaction range $\xi_{\rm int}$ of the exponentially decaying component of $J_{j,l}^{\rm (ions)}$. (c) Log-log plot of the survival probability P as a function $1/\xi_{\rm loc}$. For $\xi_{\rm loc} \to 1$, $P \sim \xi_{\rm loc}^{-\beta}$ with $\beta \simeq 3.8$, consistent with the prediction (17). We take $\delta_{N/2}/t_C = 1/3$, $N = 1000$, and values of η in the interval 0.13–0.5, for $\phi = 3\pi/4$.

Fig. 2(a), along with the corresponding interaction range [cf. Fig. 2(b)].

The localization enhancement could be actually measured in an experiment. The idea is to unveil the existence of the edge state by studying the dynamics of a single excitation at the boundary [14,15]. To detect an edge state located at, e.g., the left end of the chain, we can prepare the "excited state" $|\psi(t=0)\rangle = |\uparrow\downarrow\downarrow\ldots\rangle$, which has a large overlap with the boundary mode, and look at its survival probability at long times, $P \equiv |\langle\psi(t)|\sigma_1^+\sigma_1^-|\psi(t)\rangle|^2$, $t \to \infty$. This quantity can be estimated as (see Ref. [39])

$$P\left(\frac{1}{\xi_{\rm loc}}\right) \simeq \left(\frac{c_1}{\xi_{\rm loc}^2} + \frac{c_2}{N}\right)^2. \qquad (17)$$

Since the overlap is appreciable only if the Hamiltonian presents an edge state, P will take negligible values except in the event of localization at the left end. The initial condition $|\psi(t=0)\rangle$ requires applying a π pulse to the leftmost ion in the chain, which in turn can be prepared in the "ground state" $|\downarrow\downarrow\downarrow\ldots\rangle$ by optical pumping [13]. Then we can switch on the Hamiltonian $H_{\rm SSH}^{\rm (ions)}$, and wait up to $t \gg \Delta_0^{-1}$, where Δ_0 is the lowest energy scale in the Hamiltonian. Finally, we can perform a fluorescence measurement of the state of the leftmost ion. We have numerically confirmed the dependence of P on $\xi_{\rm loc}$ [cf. Eq. (17)] in Fig. 2(c). Deviations from the power law $P \simeq \xi_{\rm loc}^{-\beta}$, with $\beta = 4$, are the consequence of finite size effects, which play a less important role when $1/\xi_{\rm loc} \ll N$.

Correlations in the many-body ground state.—So far we have been dealing with the single-excitation subspace. Nevertheless, we expect that some localization at the edges features as well in the ground state of the many-body Hamiltonian (7). In a finite chain, states localized at each end hybridize to give rise to solutions that have support at the left and right boundaries. We expect that the correlations between the ends are zero if there is no localization at the edges whereas they must have a nonzero value otherwise, a result that has been established for the SSH model [24]. We illustrate this fact in Fig. 3, where we have computed $\langle\sigma_1^z\sigma_N^z\rangle$ as a function of the dimerization for both $H_{\rm SSH}$ and $H_{\rm SSH}^{\rm (ions)}$. The correlations in the original SSH model are non-zero for $\delta > 0$ as expected. This holds qualitatively true for $H_{\rm SSH}^{\rm (ions)}$ as well. Indeed, in the regime of short range of the interactions the correlations are larger than those of the original SSH model, which is consistent with the enhanced localization length predicted in the one-excitation subspace (cf. Fig. 2). Conversely, we observe a degradation of the correlations in the long-range interaction regime; i.e., for $\delta_{N/2} \to 0$ there is a decrease in the localization effect. This result is a consequence of the mixing—induced by the interactions—of the single-particle edge states with the bulk modes. To quantify this effect we express our generalized SSH model in terms of Jordan-Wigner fermions as $H_{\rm SSH}^{\rm (ions)} = \sum_{l>j}^N 2J_{j,l}^{\rm (ions)}\mathcal{J}_{j,l}^{\pi/2}(c_j^\dagger K_{j,l}c_l + c_jK_{j,l}c_l^\dagger)$, where $K_{j,l} \equiv \prod_{m=j}^{l-1}(1-2c_m^\dagger c_m)$. We neglect terms for which $|j-l| \geq 3$ and recast this problem as $H_{\rm SSH}^{\rm (ions)} \simeq H_0 + H_{\rm int}$, where $H_0 = \sum_{j=1}^N(J_j^{(1)}c_j^\dagger c_{j+1} + J_j^{(2)}c_j^\dagger c_{j+2} + {\rm H.c.})$, with $J_j^{(\alpha)} = 2J_{j,j+\alpha}^{\rm (ions)}\mathcal{J}_{j,j+\alpha}^{\pi/2}$ and,

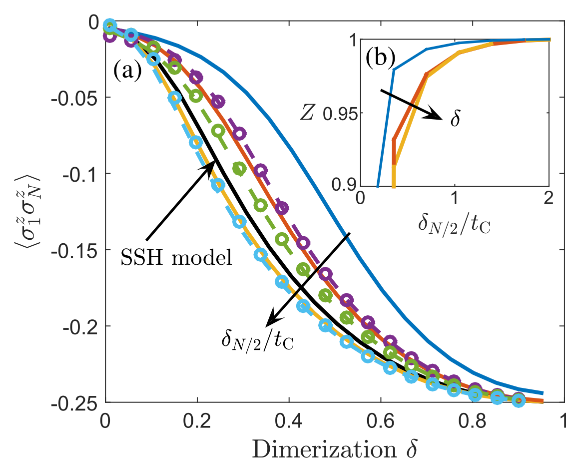

FIG. 3. (a) Correlations $\langle\sigma_1^z\sigma_N^z\rangle$ for $N = 16$, $\phi = 3\pi/4$ and using η to tune the dimerization. The arrow shows the direction of the decreasing range of the interactions, or increasing detuning from the bottom of the motional band. We have plotted curves for $\delta_{N/2}/t_C = 0.5$, 1, and 10. The solid lines represent the exact result from Hamiltonian (7), the dashed lines the results from the truncated Hamiltonian (see Ref. [39]), and the circles correspond to the predictions of the HF approximation. (b) Value of the parameter Z for different interaction ranges and $\delta = 0.1$, 0.3, 0.5 from bottom to top.

$$H_{\rm int} = -2\sum_{j=1}^{N} J_j^{(2)}(c_j^\dagger c_{j+1}^\dagger c_{j+1}c_{j+2} + {\rm H.c.}). \quad (18)$$

We deal with the interaction term within the Hartree-Fock approximation [47], which renders a simplified Hamiltonian quadratic in fermion operators (see Ref. [39])

$$H_{\rm HF} = \sum_{\mu=1}^{N} \varepsilon_\mu c_\mu^\dagger c_\mu - 2\sum_{\mu,\mu'=1}^{N} V_{\mu,\mu'} c_\mu^\dagger c_{\mu'}. \quad (19)$$

$H_{\rm HF}$ is expressed in terms of the eigenstates of H_0, which correspond to the solutions of the Hamiltonian in the one-excitation subspace [cf. Eq. (10)], that is, $c_j = \sum_{\mu=1}^{N} M_{j,\mu} c_\mu$. The one-body edge states are eigenstates of H_0 and $V_{\mu,\mu'}$ induces the mixing of these states with the bulk modes. We quantify this effect with a parameter Z, which measures the overlap between the unperturbed boundary modes and the corresponding states in the presence of interaction, and which can be estimated by elementary perturbation theory as $Z \simeq 1 - \sum_{\mu\neq E.S.}^{N} 4|V_{E.S.,\mu}|^2/(\varepsilon_{E.S.} - \varepsilon_\mu)^2$. We show this quantity as a function of the range of interactions in the inset of Fig. 3. Accordingly, when $\delta_{N/2} \to 0$ the fidelity drops significantly, signaling the decay of the edge modes into the continuum of the states in the bulk. Finally the average $\langle \sigma_1^z \sigma_N^z \rangle$ can be measured in an experiment by detecting the photoluminescence from individual ions at the ends of the chain (e.g., by electron-shelving techniques [25]).

Conclusions and outlook.—In this work we have established the feasibility of implementing a topological insulator with trapped-ion quantum matter. We have shown that the edge states get more localized because of the long-range interactions in ion chains, and that the localized solutions survive to the interactions in the many-body ground state. An immediate extension of this work would consist in the computation of the Zak phase of the many-body ground state, and establishing the symmetries of the model, to shed light on a prospective bulk-edge correspondence in this system. Our ideas could be extended to systems of cold atoms [48,49] or superconducting qubits [50], where dipolar interactions are available.

We are greatly indebted to Alejandro Bermúdez for very useful discussions. P. N. thanks Hiroki Takahashi for his feedback on the implementation. Our research has received funding from the People Programme (Marie Curie Actions) of the European Union's Seventh Framework Programme (FP7/2007-2013) under REA Grant Agreement No. PCIG14-GA-2013-630955.

*pedro.nevado.serrano@gmail.com
†D.Porras@Sussex.ac.uk

[1] A. Kitaev, Ann. Phys. (N. Y.) **303**, 2 (2003).
[2] C. Nayak, S. H. Simon, A. Stern, M. Freedman, and S. Das Sarma, Rev. Mod. Phys. **80**, 1083 (2008).
[3] M. Z. Hasan and C. L. Kane, Rev. Mod. Phys. **82**, 3045 (2010).
[4] J. E. Moore, Nature (London) **464**, 194 (2010).
[5] X.-L. Qi and S.-C. Zhang, Rev. Mod. Phys. **83**, 1057 (2011).
[6] B. A. Bernevig, *Topological Insulators and Topological Superconductors* (Princeton University Press, Princeton, NJ, 2013).
[7] M. König, S. Wiedmann, C. Brüne, A. Roth, H. Buhmann, L. W. Molenkamp, X.-L. Qi, and S.-C. Zhang, Science **318**, 766 (2007).
[8] Y. L. Chen, J. G. Analytis, J.-H. Chu, Z. K. Liu, S.-K. Mo, X. L. Qi, H. J. Zhang, D. H. Lu, X. Dai, Z. Fang, S. C. Zhang, I. R. Fisher, Z. Hussain, and Z.-X. Shen, Science **325**, 178 (2009).
[9] I. Bloch, J. Dalibard, and W. Zwerger, Rev. Mod. Phys. **80**, 885 (2008).
[10] M. Lewenstein, A. Sanpera, V. Ahufinger, B. Damski, A. Sen(De), and U. Sen, Adv. Phys. **56**, 243 (2007).
[11] D. Porras and J. I. Cirac, Phys. Rev. Lett. **92**, 207901 (2004).
[12] A. Friedenauer, H. Schmitz, J. T. Glueckert, D. Porras, and T. Schaetz, Nat. Phys. **4**, 757 (2008).
[13] C. Schneider, D. Porras, and T. Schaetz, Rep. Prog. Phys. **75**, 024401 (2012).
[14] P. Jurcevic, B. P. Lanyon, P. Hauke, C. Hempel, P. Zoller, R. Blatt, and C. F. Roos, Nature (London) **511**, 202 (2014).
[15] P. Richerme, Z.-X. Gong, A. Lee, C. Senko, J. Smith, M. Foss-Feig, S. Michalakis, A. V. Gorshkov, and C. Monroe, Nature (London) **511**, 198 (2014).
[16] S. Ryu and Y. Hatsugai, Phys. Rev. Lett. **89**, 077002 (2002).
[17] F. Grusdt, M. Höning, and M. Fleischhauer, Phys. Rev. Lett. **110**, 260405 (2013).
[18] Z.-X. Gong, M. F. Maghrebi, A. Hu, M. L. Wall, M. Foss-Feig, and A. V. Gorshkov, Phys. Rev. B **93**, 041102 (2016).
[19] K. Patrick, T. Neupert, and J. K. Pachos, Phys. Rev. Lett. **118**, 267002 (2017).
[20] A. Bermudez, L. Tagliacozzo, G. Sierra, and P. Richerme, Phys. Rev. B **95**, 024431 (2017).
[21] W. P. Su, J. R. Schrieffer, and A. J. Heeger, Phys. Rev. Lett. **42**, 1698 (1979).
[22] W. P. Su, J. R. Schrieffer, and A. J. Heeger, Phys. Rev. B **22**, 2099 (1980).
[23] A. J. Heeger, S. Kivelson, J. R. Schrieffer, and W. P. Su, Rev. Mod. Phys. **60**, 781 (1988).
[24] L. Campos Venuti, S. M. Giampaolo, F. Illuminati, and P. Zanardi, Phys. Rev. A **76**, 052328 (2007).
[25] D. Leibfried, R. Blatt, C. Monroe, and D. Wineland, Rev. Mod. Phys. **75**, 281 (2003).
[26] A. Sørensen and K. Mølmer, Phys. Rev. Lett. **82**, 1971 (1999).
[27] E. Solano, R. L. de Matos Filho, and N. Zagury, Phys. Rev. A **59**, R2539 (1999).
[28] C. Sackett, D. Kielpinski, B. King, C. Langer, V. Meyer, C. Myatt, M. Rowe, Q. Turchette, W. Itano, D. Wineland, and C. Monroe, Nature (London) **404**, 256 (2000).
[29] P. J. Lee, K. Brickman, L. Deslauriers, P. C. Haljan, L.-M. Duan, and C. Monroe, J. Opt. B: Quantum Semiclassical Opt. **7**, S371 (2005).
[30] X. L. Deng, D. Porras, and J. I. Cirac, Phys. Rev. A **72**, 063407 (2005).

[31] P. Nevado and D. Porras, Phys. Rev. A **93**, 013625 (2016).
[32] S. Fernández-Lorenzo, J. J. García-Ripoll, and D. Porras, New J. Phys. **18**, 023030 (2016).
[33] W. Paul, Rev. Mod. Phys. **62**, 531 (1990).
[34] J. Chiaverini, R. B. Blakestad, J. Britton, J. D. Jost, C. Langer, D. Leibfried, R. Ozeri, and D. J. Wineland, Quantum Inf. Comput. **5**, 419 (2005).
[35] S. Seidelin, J. Chiaverini, R. Reichle, J. J. Bollinger, D. Leibfried, J. Britton, J. H. Wesenberg, R. B. Blakestad, R. J. Epstein, D. B. Hume, W. M. Itano, J. D. Jost, C. Langer, R. Ozeri, N. Shiga, and D. J. Wineland, Phys. Rev. Lett. **96**, 253003 (2006).
[36] J. P. Home, D. Hanneke, J. D. Jost, J. M. Amini, D. Leibfried, and D. J. Wineland, Science **325**, 1227 (2009).
[37] H. J. Weber and G. B. Arfken, *Essential Mathematical Methods for Physicists* (Elsevier, Academic Press, New York, 2004).
[38] J. Asbóth, L. Oroszlány, and A. Pályi, *A Short Course on Topological Insulators: Band Structure and Edge States in One and Two Dimensions* (Springer International Publishing, New York, 2016).
[39] See Supplemental Material at http://link.aps.org/supplemental/10.1103/PhysRevLett.119.210401 for a discussion of the chiral symmetry, the continuum limit, the survival probability, and the Hartree-Fock theory, which includes Refs. [40–45].
[40] R. Blatt and C. F. Roos, Nat. Phys. **8**, 277 (2012).
[41] K. Kim, M.-S. Chang, S. Korenblit, R. Islam, E. E. Edwards, J. K. Freericks, G.-D. Lin, L.-M. Duan, and C. Monroe, Nature (London) **465**, 590 (2010).
[42] R. Resta, Rev. Mod. Phys. **66**, 899 (1994).
[43] H. Takayama, Y. R. Lin-Liu, and K. Maki, Phys. Rev. B **21**, 2388 (1980).
[44] E. Lieb, T. Schultz, and D. Mattis, Ann. Phys. (N.Y.) **16**, 407 (1961).
[45] J. J. Sakurai and J. J. Napolitano, *Modern Quantum Mechanics* (Pearson, San Francisco, 2011).
[46] J. Zak, Phys. Rev. Lett. **62**, 2747 (1989).
[47] A. Altland and B. D. Simons, *Condensed Matter Field Theory*, 2nd ed. (Cambridge University Press, Cambridge, England, 2010).
[48] I. Bloch, J. Dalibard, and S. Nascimbene, Nat. Phys. **8**, 267 (2012).
[49] J. Ruostekoski, J. Javanainen, and G. V. Dunne, Phys. Rev. A **77**, 013603 (2008).
[50] M. Dalmonte, S. I. Mirzaei, P. R. Muppalla, D. Marcos, P. Zoller, and G. Kirchmair, Phys. Rev. B **92**, 174507 (2015).